



Removal of Reactive Dyes From Aqueous Solution by Adsorption onto Alfa Fibers powder

S. Fettouche^{1,2}, M. Tahiri¹, R. Madhouni², O. Cherkaoui^{2*}

¹University Hassan II, Faculty of Sciences Ain Chock, Department of Chemistry, Laboratory Interface Materials Environment, Casablanca, Morocco

²Higher School of Textile and Clothing Industries, Laboratory REMTEX, Casablanca, Morocco

Received 20 March 2014; Revised 6 November 2014; Accepted 11 November 2014.

*Corresponding Author. E-mail: cherkaoui@esith.ac.ma ; Tel: (+212667459119).

Abstract

The absorbent Alfa fibers powder was used for its low cost, available and natural for removal of reactive textile dyes (reactive red 23 (RR-23) and reactive blue 19 (RB-19)) from aqueous solution. The absorbent Alfa fibers powder was obtained from leaf of *Stippa Tenacissima L* crushed and screened with a particle size less than < 2mm. Batch experiments were carried out for sorption kinetics and isotherms. Operating variables studied were pH, treatment time, temperature, dye and adsorbent concentrations. The adsorption parameters were determined based on Langmuir and Freundlich isotherm models. These parameters were obtained from the equilibrium adsorption data for the two reactive dyes. While the kinetics and thermodynamic parameters were used to establish the adsorption mechanism. As an adsorbent, Alfa fibers powder have a preference for Reactive Red 23, retaining up to 34.13 mg/g at 22°C, whereas a retention of only 11.33 mg/g at 22°C has been achieved by Reactive blue 19. Besides that, the thermodynamic study showed that the dye adsorption onto absorbent Alfa fibers powder was favourable, endothermic and spontaneous.

Keywords: adsorption kinetics, adsorption isotherm, alfa fibers powder, leaf of *Stippa Tenacissima L*, RR-23 dye, RB-19 dye

1. Introduction

Synthetic dyes are extensively used in the textile industry. Due to inefficiencies of the industrial dyeing process, some of the used dyes are lost in the effluents of textile units, rendering them highly coloured [1,2]. The colors disturb the biological activities in water bodies and are toxic, mutagenic and carcinogenic. They can threaten aquatic life by causing disturbances in the function of kidneys, reproductive system, brain and central nervous system [3]. The industrial effluents containing dyes need to be treated before being released back into the environment [4]. Several biological, physical and chemical methods have been used for the treatment of industrial textile wastewater including microbial biodegradation, membrane filtration, oxidation and ozonation [5]. Conventional treatments are often disadvantageous to remove reactive dyes owing to their high solubility and low biodegradability [6]. Moreover, many of these technologies are cost prohibitive, especially when applied for treating large waste streams. Consequently, adsorption techniques seem to have the most potential for future use in industrial wastewater treatment because of their proven efficiency in the removal of organic and mineral pollutants and for economic considerations [7,8]. Hence, adsorption is recommended as it is viable means for reactive dye removal. The most widely used adsorbent for this purpose is activated carbon, but its overlying cost [9] has led to look for cheaper alternative materials such as orange and banana peels [10], agricultural residues [11], fibrous biomass [12] and Chitosan [13]. The objective of the present study is to evaluate the feasibility of absorbent Alfa fibers powder (AFP) to remove separately reactive red 23 dye (RR-23) and reactive blue 19 dye (RB-19) from aqueous solutions. The effects of various operating parameters on the adsorption such as initial pH, dye concentration, adsorbent concentrations and adsorption temperature were investigated in controlled batch experiments. Langmuir and Freundlich isotherm models were used for describing the relationship between the amount of adsorbed dye and adsorbent in the solution. Finally, the equilibrium, kinetic and thermodynamical parameters were also evaluated.

2. Materials and methods

2.1. Preparation of the absorbent AFP

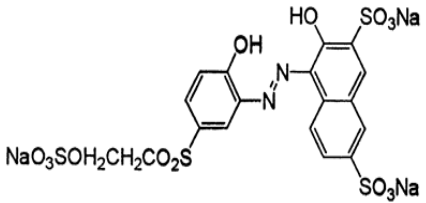
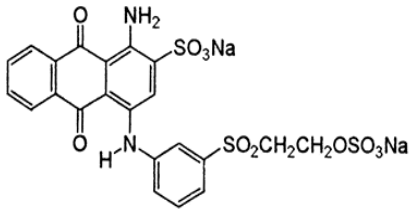
The absorbent AFP was obtained from the leaves of the wild plant *Stippa tenacissima* L by grinding and simultaneously screening to have a size of less than <2 mm by (Polymix PX-MFC 90 D) type mill. The obtained powder was washed by Soxhlet extractor with a solution of NaOH, 1 mol.l⁻¹ for 4h. This pretreatment aimed to reduce the level of waxes and lignin and increase the absorption rate of the powder. The powder was transferred to a Buchner funnel on a Whatman n°1 filter paper and washed with distilled water until neutral pH was reached and then dried in an oven at 60°C for 12 h to a constant weight. The chemical structure of AFP was characterized using an FT-IR spectrometer (FT-IR Nicolet IS 10) and scanning electron microscope (Hitachi S-2360N SEM operating at 20kV). The initial concentration of the adsorbent is 0.03 g/ml.

The chemical composition of leaves of the wild plant *Stippa tenacissima* L is mainly composed of cellulose (43-47%), lignin (18-24%), hemicellulose / Pectin (22-28%), waxes (0-5%) and ash (2 - 5%) [14].

2.2. Dyes (adsorbate systems)

Two commercial dyes (C.I. Reactive Red 23-16202 (RR-23) and (C.I. Reactive blue 19-61200 (RB-19)), whose structures are shown in table 1, were obtained from Dye Star Company. Reactive dyes have mainly a functional group (triazinyl, vinyl sulphone, etc.) that makes available to make a bond (covalent in general) with fabric. The dyes were used without further purification. The stock solution was prepared by dissolving 1g of each reactive dye in 1l distilled water. For the present analysis, the dye solutions with different concentrations were prepared by diluting the stock solution with distilled water. Initial pH was adjusted by admixing dilute HCl or NaOH solutions. The concentration of the dye solution was determined by using UV-vis spectrophotometer (Thermo Scientific Evolution 300) at their maximum wavelengths, respectively. The maximum absorption wavelength of the dye (λ_{max}) was determined by absorbance spectrum detection between 200 nm to 800 nm using the same UV-Vis spectrophotometer. The curve of absorption shows λ_{max} of 511 nm for RR-23 and λ_{max} of 592 nm for RB-19 respectively. For controlling the accuracy of spectrophotometric results, calibration curve was drawn.

Table 1: Basic properties of reactive RR-23 and reactive RB-19 dyes

<p>Azo dye with functional group vinyl sulphone</p> 	<ul style="list-style-type: none"> • Commercial name : Remazol Red 3 B • C.I. Reactive Red 23, C.I.16202 • CAS : 12769-07-2 • Molecular formula: C₁₈H₁₃N₂Na₃O₁₄S₄, • Molecular weight: 678.53 g. mol⁻¹ • λ_{max} : 511 nm
<p>Anthraquinone dye with functional group vinyl sulphone</p> 	<ul style="list-style-type: none"> • Commercial name : Remazol Brilliant Blue R • C.I. Reactive Blue 19, C.I.61200 • CAS : 2580-78-1 • Molecular formula: C₂₂H₁₆N₂Na₂O₁₁S₃ • Molecular weight: 626.55 g. mol⁻¹ • λ_{max} : 592 nm

2.3. Adsorption experiments

All the adsorption experiments were carried out by batch technique. The kinetic adsorption studies were performed at different doses of adsorbent, pH, temperature and dye concentrations. The initial concentrations of reactive dye in the experiments were selected in the range of 25 to 100 mg/l. The dye solution (100 ml) of desired concentration at neutral pH was taken in Al-covered glass vials and agitated with a known weight of absorbent AFP at room temperature (22°C) in a shaker set at 150 rpm for desired time periods.

The preliminary kinetic experiments revealed that 90 min was long enough to achieve the equilibrium. Therefore, a treatment time of 90 min was selected for the equilibrium tests. The solution pH was carefully adjusted by adding a small amount of HCl and NaOH solutions (0.1mol/l), which concentration was measured by using a pH meter (Thermo Scientific Orion 4 star pH-ISE). At the end of adsorption tests, samples were filtered by filter paper having 0.45 μ m pore size and the filtrate was analyzed. The concentrations of residual dye were determined using the above mentioned UV-Vis spectrophotometer corresponding to λ_{max} = 511 nm for RR-23 and λ_{max} = 592 nm for RB-19. Blank solution with no dye was used for each series of experiments. Dilutions were carried out when measurement exceeded the linearity of the

calibration curve. The sorption capacities at equilibrium and dye removal efficiency were calculated from the mass balance Equation (1):

$$q_e = \frac{V}{M} \times (C_0 - C_e) \quad (1)$$

Where C_e and C_0 are the equilibrium and the initial concentrations of dye (mg/l) respectively, q_e is the equilibrium dye concentration on adsorbent (mg/g), V is the volume of dye solution (l), M is the mass of adsorbent (g). The effect of adsorbent dosage was studied by changing the amount of adsorbent AFP mass from 1 to 5g.

3. Results and discussion

3.1. Characterization of the adsorbent

The spectra of AFP before adsorption (AFP-BA) and after adsorption (AFP-AA) were shown in figure 1. One could find that the most significant bands were in the regions of 3373, 2958, 1737, 1647 and 1048 cm^{-1} for AFP-BA. The broad band at 3373 cm^{-1} was investigated to absorbed water. A weak absorption at 2958 cm^{-1} was usually ascribed to the alifatic groups (asymmetrical and symmetrical stretch of CH_3). The band located in 1737 cm^{-1} of AFP-BA corresponded to an aromatic carbon or carbonyls. These band shifted to heigher frequencies after adsorbing the dye, which indicated an aromatic carbon or carbonyls could combine with the dye molecules on the surface of adsorbent. The band at 1048 cm^{-1} of AFP-BA may belong to C-O stretching in alcohol or ether or hydroxyl groups. It could be seen that the absorbance peaks in AFP-AA shifted to 1056 cm^{-1} the above results indicated that functional groups on the surface of AFP affected the absorption process [15-16].

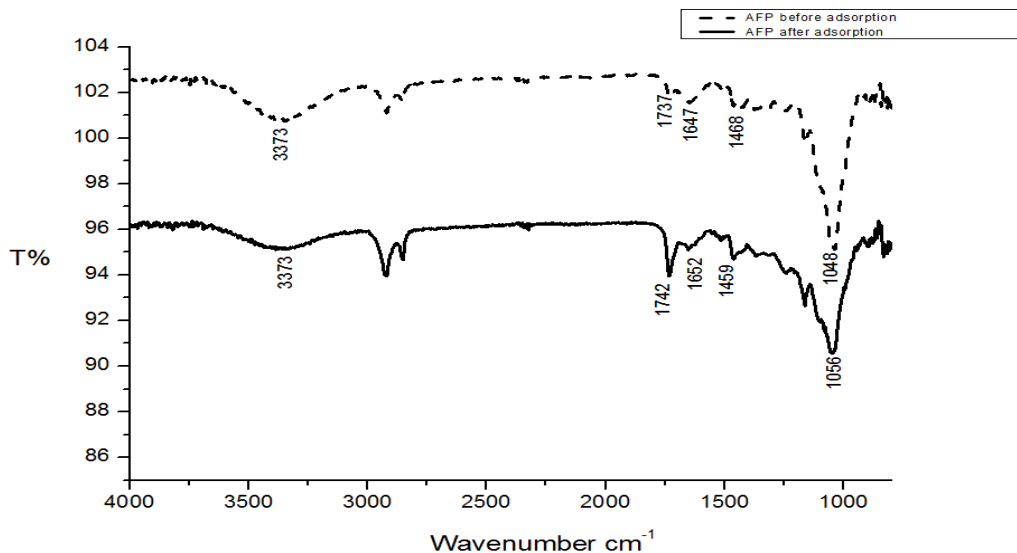


Figure 1: FT-IR spectrum of AFP-BA and AFP-AA of dye

The SEM images of AFP before adsorption are shown in figure 2. The adsorbent had an irregular and porous surface, pores of different size (from 2 μm to 20 μm) and different shape could be observed, most of the pores are distributed at the surface of the surround, revealing the potential adsorption powder due to providing high internal surface area [17].

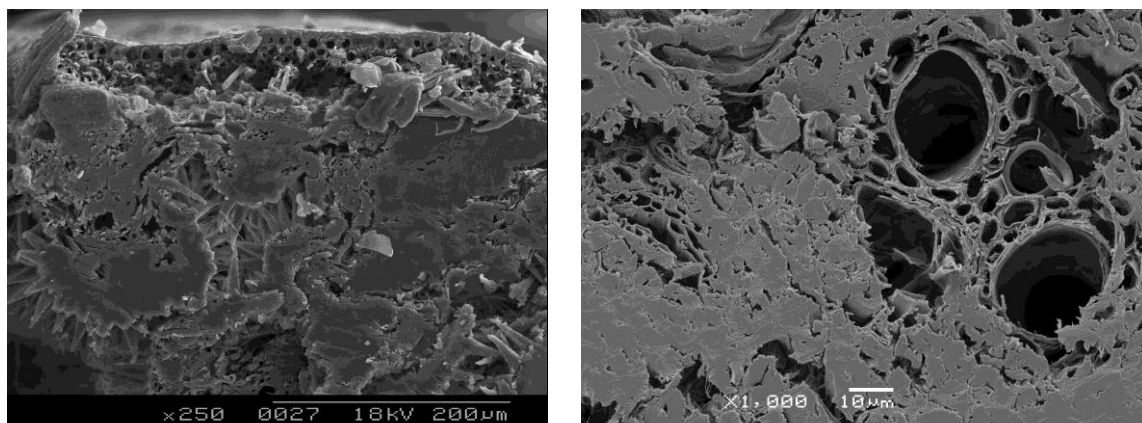


Figure 2: SEM image of AFP before adsorption

3.2. Effect of pH solution

The initial pH value of the solution is an important factor during sorption. The effect of pH on the amount of dye removal was analyzed by UV-Vis spectrophotometer over the pH range from 2 to 6 and the results are presented in Figure 3. As shown, the adsorption capacity increases with decreasing pH. Therefore the maximum absorption capacity was reached at pH 2 for both RR-23 and RB-19 dyes, lower adsorption at pH >4 is provable due to the presence of OH⁻ ions competing with dye anions for adsorption sites. As the pH of the system decrease and number of positively charged surface sites decrease and the number of positively charged surface sites on the adsorbent favours the adsorption of the anions due to electrostatic attraction. A similar result was observed for the adsorption of dye Acid violet 17 by cellulose adsorbent as banana pith [18] and orange peel [19].

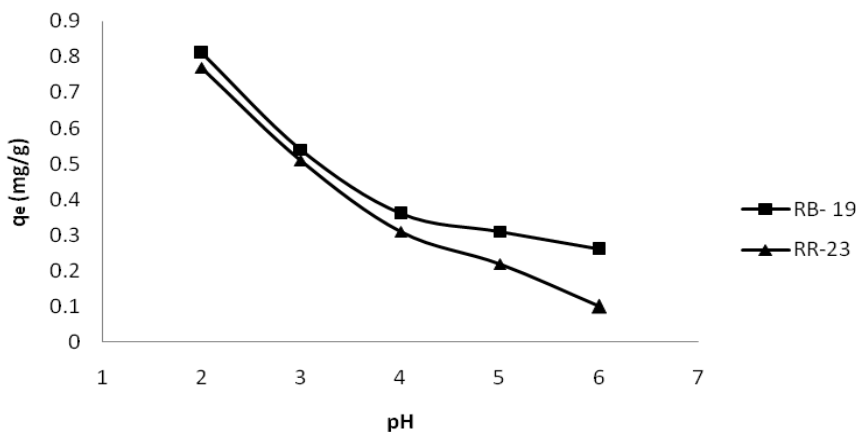


Figure 3: Effect of initial pH on adsorption capacity (Solid/Liquid ratio= 0.03g/ml, [RR-23]=25 mg/l, [RB-19]=25 mg/l, T=22°C , 150 rpm)

3.3. Treatment time

The effect of treatment time on the removal efficiency is presented in Figure 4. The results showed that with increasing reaction time, efficiency of adsorption increased and maximum adsorption achieved in 60 min for RR-23 dye ($q_e = 0.82$ mg/g) and 30min for RB-19 dye ($q_e = 0.77$ mg/g). After this time, no notable increase was observed. Moreover, the extension of treatment time up to 90 min does not lead to a significant improvement in removal rate of dyes. We note that the RB-19 dye reacts faster and more efficiently than the RR-23 dye with the adsorbent AFP.

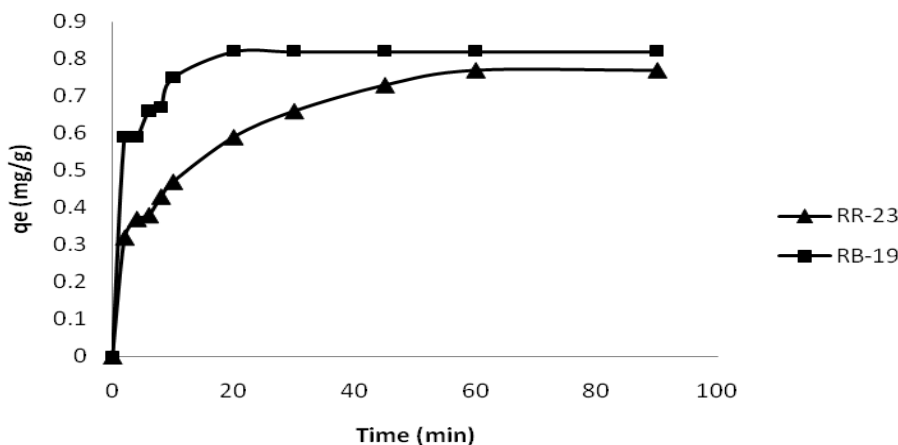


Figure 4: Dye adsorption as a function of time (Solid/Liquid ratio= 0.03g/ml, [RR-23]= 25 mg/l, [RB-19]=25 mg/l, T=22 °C , pH=2 , 150 rpm)

3.4. Effect of the mass of the adsorbent

The removal of dye increased with the amount of the adsorbent AFP ranging from 0.01 to 0.05 g/ml of colored solution, but the adsorption capacity decreased and reached its maxima retention as shown in Figure 5. Theoretically, the number of sorption sites available increases by increasing the amount of adsorbent, this enhances the removal efficiency of the two reactive dyes. The decrease in adsorption capacity can be attributed

to the fact that some of the sorption sites remain unsaturated during the sorption process. Similar results are mentioned by other researchers [20,21].

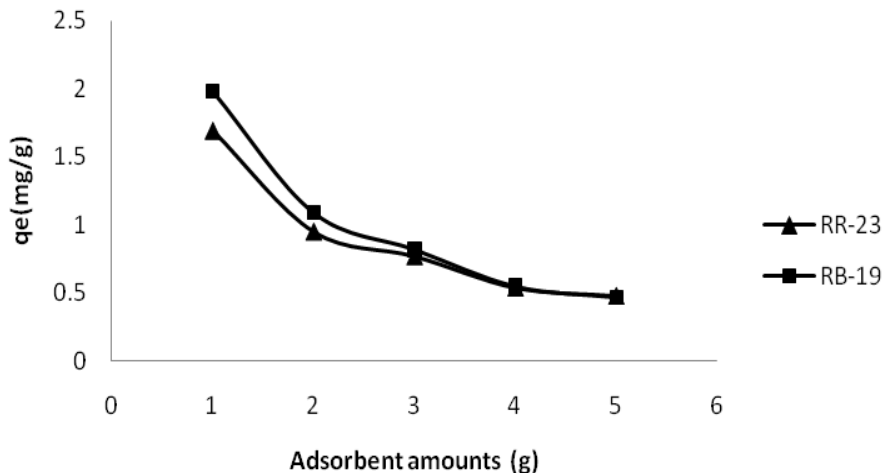


Figure 5: Effect of the mass of the adsorbent ([RR 23]= 25 mg/l, [RB-19]=25 mg/l, T=22°C , pH=2 , 150 rpm , treatment time: RR-23=60 min and RB-19=30 min)

3.5. Effect of temperature

The data of dye adsorption onto adsorbent AFP obtained from UV-vis spectrophotometer indicates a change in dye removal efficiency at different temperature. This effect is shown in Figure 6. The improvement of the sorption capacity at equilibrium for two reactive dyes shows that the increased temperature enhances the removal of dye from aqueous solution onto adsorbent AFP. Indeed, by increasing the temperature from 25 to 50 °C, the equilibrium capacity of dye increased from 0.76 to 0.79 mg/g for RR-23 dye and from 0.81 to 0.83 mg / g for RB-19 dye [22]. As the temperature increases, rate of diffusion of adsorbate dyes molecules across external boundary layer and internal pores of adsorbent particle increases [23]. Changing the temperature will change the equilibrium capacity of the adsorbent for particular adsorbate.

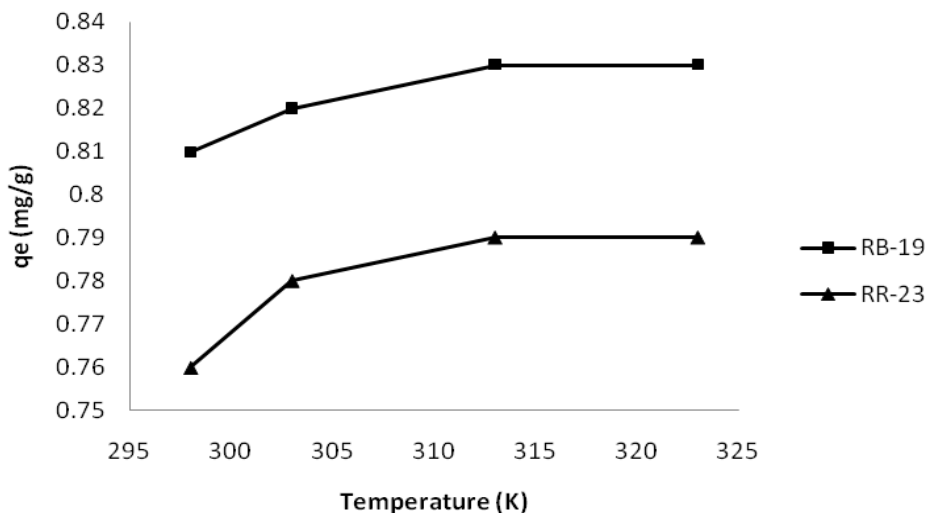


Figure 6.: Effect of temperature on the dye concentration (Solid/Liquid ratio= 0.03g/ml, [RR-23]= 25 mg/l, [RB-19]=25 mg/l, pH=2 , 150 rpm, treatment time: RR-23 = 60 min, RB-19= 30 min)

3.6. Effect of the initial concentration of dye

Studies were conducted starting from initial concentration of 25 and checked at 100 mg/l at 22°C. Figure 7 shows that the amount of adsorbed dye increased with time. Sorption capacitive (q_e) increased from 0.69 to 2.2 mg/g for RR-23 dye and 0.75 to 3.03 mg/g for RB-19 dye until saturation.

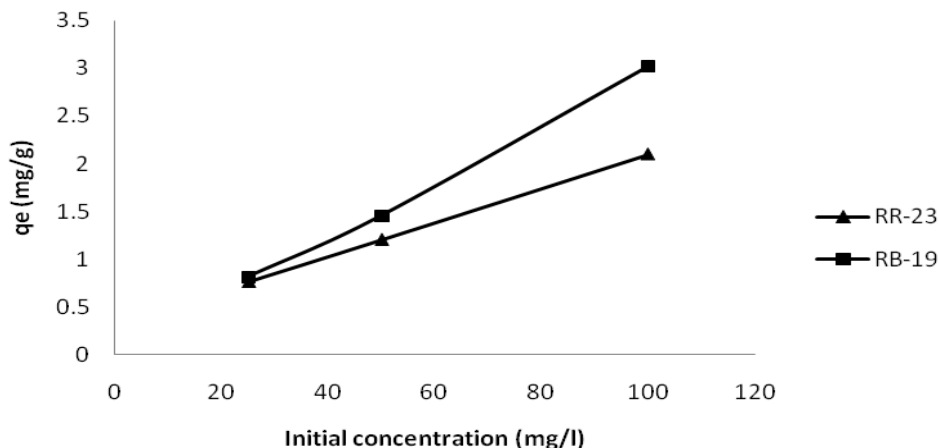


Figure 7: Effect of initial concentration of dye (Solid/liquid ratio= 0.03g/ml, pH=2, 150 rpm, treatment time: RR-23 = 60 min, RB-19=30 min)

3.7. Thermodynamic studies

In order to qualify the adsorptive removal process, thermodynamic factors including the adsorption change in Gibbs free energy ΔG° (kJ/mol), enthalpy ΔH° (kJ/mol), and entropy ΔS° (J/mol.K) were calculated by using the van't Hoff equation with the values of K_d obtained at different temperatures [24] :

$$K_d = \frac{q_e}{C_e} \quad \text{and} \quad \Delta G^\circ = -RT \ln(K_d) \quad (2)$$

$$\ln(K_d) = \frac{\Delta S^\circ}{R} - \frac{\Delta H^\circ}{RT} \quad (3)$$

Where K_d is the adsorption distribution coefficient, R is the universal gas constant (8.314 J/mol/K) and T is the absolute temperature (K). The experimented temperature range was from 25°C (298K) to 50°C (323K). The Gibbs free energy indicates the degree of spontaneity of the sorption process and a negative value reflects favourable sorption. ΔH° and ΔG° values, recorded in Table 2, were obtained from the slope and intercept of a plot of $\ln K_d$ versus $1/T$ (K^{-1}).

Table 2: Thermodynamic parameters

ΔS° (J.mol ⁻¹ .K ⁻¹)		ΔH° (KJ.mol ⁻¹)		ΔG° (KJ.mol ⁻¹)		T(K)
RB-19	RR-23	RB-19	RR-23	RB-19	RR-23	
60.06	22.61	16.470	6.19	-1.27	-0.45	298
				-1.84	-0.85	303
				-2.51	-0.8	313
				-2.78	-1.14	323

The negative value of Gibb's free energy (ΔG°) indicated that the adsorption was spontaneous for both RR-23 and RB-19 reactive dyes [25]. The results showed that the adsorbent AFP was suitable for the removal of the reactive dyes from the aqueous solutions. The positive value of enthalpy (ΔH°) indicated that the adsorption of the selected dyes were endothermic. Furthermore, the positive (ΔS°) indicates that the degrees of freedom increased at the solid – liquid interface during adsorption of reactive dyes onto adsorbent AFP. [26] also reported a similar observation for the adsorption of Reactive Orange 4 by activated carbon prepared from Thevetia Peruviana.

3.8. Sorption equilibrium modeling

The adsorption isotherm indicates how the adsorption molecules distribute between the liquid phase and solid phase when the adsorption reaches an equilibrium state. Adsorption isotherms describe the interaction of adsorbate molecules with adsorbent surface. In this study, Langmuir and Freundlich isotherms were applied for the treatment of the equilibrium adsorption data. The applicability of the isotherm equation is compared by judging the correlation coefficients r^2 .

3.8.1. Langmuir model:

The Langmuir adsorption isotherm is the best known linear template for monolayer adsorption on the homogeneous surface and is used to determine the adsorption parameters. Langmuir template is represented by (4):

$$\frac{C_e}{q_e} = \frac{C_e}{q_m} + \frac{1}{K_L q_m} \quad (4)$$

Where q_e (mg/g) is a constant related to the area occupied by a monolayer of adsorbate, reflecting the maximum adsorption capacity. C_e is the equilibrium concentration of adsorbate and K_L (l/mg) is a direct measure of the intensity of the sorption. Figure 8 described the plots of $1/q_e$ against $1/C_e$ using linear regression analysis. The constants q_m and K_L (Table 3) were determined from the intercept and slope of the linear plots. The essential features of the Langmuir isotherm may be expressed in terms of equilibrium parameter R_L , which is a dimensionless constant referred to as separation factor or equilibrium parameter [27].

$$R_L = \frac{1}{(1+K_L C_0)} \quad (5)$$

Where:

C_0 = initial concentration

K_L = the constant related to the energy of adsorption (Langmuir Constant). R_L value indicates the adsorption nature to be either unfavourable if $R_L > 1$, linear if $R_L = 1$, favourable if $0 < R_L < 1$ and irreversible if $R_L = 0$. From the data calculated in table 3, the R_L is greater than 0 but less than 1 indicating that Langmuir isotherm is favourable. From this research work, The maximum adsorption capacity of the adsorbent for RR-23 and RB-19 was calculated from the Langmuir isotherm and found to be 34.13 and 11.33 mg/g, respectively, K_L (Langmuir isotherm constant) is $4.9 \cdot 10^{-3}$ and 0.03 L/mg for RR-23 and RB-19, respectively, and R_L (the separation factor) is 0.47 and 0.36 for RR-23 and RB-19, respectively, indicating that the equilibrium sorption was favourable.

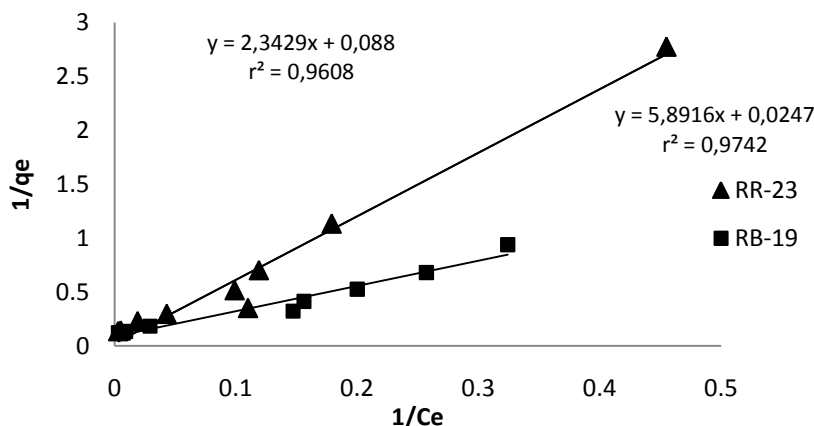


Figure 8: Linear Langmuir model for RR-23 and RB-19 dyes (Solid/Liquid ratio= 0.03g/ml, T=22°C, pH=2, treatment time: RR-23 = 60 min, RB-19=30 min)

3.8.2. Freundlich model

The linearized form of the Freundlich isotherm equation is given by (6):

$$\ln q_e = \ln K_F + \frac{1}{n} \ln C_e \quad (6)$$

Where K_F (mg/g) is the Freundlich constant and n the constant related to adsorption intensity. A plot of $[\ln(q_e)]$ against $[\ln(C_e)]$ would give the value of n and K_F , from the slope and the intercept, respectively. The Freundlich isotherm described as a fairly satisfactory empirical isotherm used for non-ideal adsorption is related to heterogeneous process as well as to multilayer adsorption. The linearized Freundlich adsorption of RR-23 and RB-19 is given in Figure 9. The magnitude of the term $(1/n)$ gives in general an indication on the suitability between adsorbent and adsorbate systems in terms of fixation degree and commodity of retention sites [28]. For $1/n=1$, the partition between the two phases is independent of the concentration. The situation $1/n < 1$ is the most common and corresponds to a normal L-type Langmuir isotherm, while $1/n > 1$ is indicative of a cooperative adsorption which involves strong interactions between the molecules of adsorbate. The Langmuir and Freundlich adsorption constants evaluated from isotherms and their correlation coefficients are presented in Table 3. It is clear that the Langmuir isotherm model provide an excellent fit to the equilibrium

adsorption data, giving correlation coefficients of 0.97 for RR-23 and 0.96 for RB-19, respectively. The value of $1/n$ is found to be below number 1 for both dyes, indicating that the adsorption of reactive dyes on adsorbent AFP is favourable. However it fits poorly to the experimental data of correlation coefficient 0.93 for RR-23 and 0.92 for RB-19. The results of isotherms are show in Table 3.

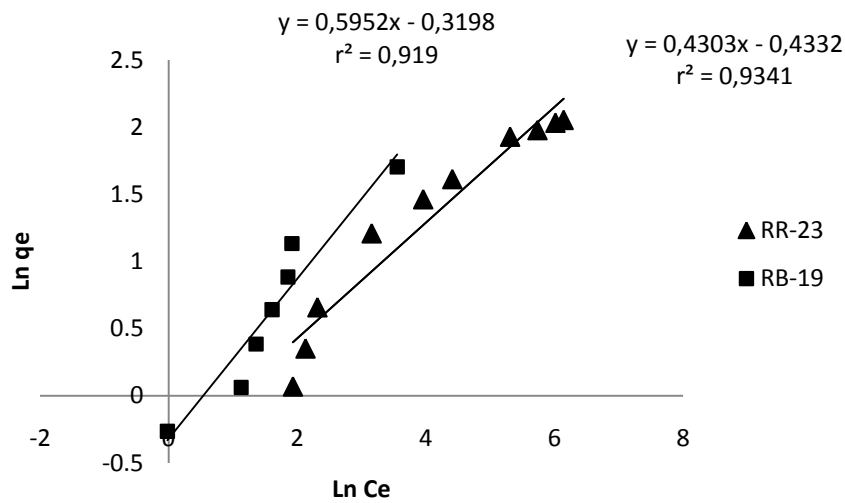


Figure 9: Freundlich linear model for RR-23 and RB-19 dyes (Solid/Liquid ratio=0.03 g/ml, T = 22°C, pH=2, treatment time: RR-23 = 60 min, RB-19=30 min)

Table 3: Equilibrium and kinetic study of RR-23 and RB-19 dyes onto adsorbent AFP

Sorption equilibrium modelling							
Dyes		Model Langmuir			Model Freundlich		
		q_m (mg/g)	K_L (l/mg)	r^2	n	K_F (mg/g)	r^2
RR-23		34.13	4.9.10 ⁻³	0.97	2.32	0.64	0.93
RB-19		11.33	0.03	0.96	1.68	0.72	0.92
Sorption kinetic modelling							
Dyes	C0 (mg/l)	Pseudo First order			Pseudo Second order		
		K_1 min ⁻¹	q_e (mg/g)	r^2	K_2 (g/mg.min)	q_e (mg/g)	r^2
RR-23	25	0.095	0.73	0.98	0.184	3.773	0.99
	50	0.06	0.95	0.94	0.221	5.912	0.99
	100	0.061	1.14	0.89	0.522	4.278	0.99
RB-19	25	0.046	1.626	0.84	0.974	0.76	0.99
	50	0.108	0.745	0.85	0.762	2.026	0.99
	100	0.123	0.409	0.99	0.504	7.056	0.99

3.9. Sorption kinetic modelling

The adsorption kinetics, as expressed in terms of the rate of up take of solute (which governs the residence time), is one of the important considerations for economical wastewater treatment applications [29]. The kinetics of reactive dyes (RR-23 and RB-19) adsorption on adsorbent AFP was evaluated with the pseudo-first order and pseudo-second order models. For the analysis of data with the first model, the linear form of Lagergren equation was used, in which integrated form can be expressed as (7) :

$$\log(q_e - q_t) = \log(q_e) - \frac{K_1}{2.203} t \quad (7)$$

With q_t and q_e are the amount adsorbed at time t and at equilibrium respectively and k_1 is the rate constant for pseudo-first order kinetic which can be calculated from the plot of $\log(q_e - q_t)$ versus time.

Since this model may not fully describe the adsorption kinetics, the pseudo-second-order equation was used. This model is often successfully applied to describe the kinetics of fixation of adsorbate on adsorbent surface. The linear and integrated form of this model can be described as (8) [30]:

$$\frac{t}{q_t} = \frac{1}{K_2 q_e^2} + \frac{1}{q_e} t \quad (8)$$

With q_t and q_e are the amount adsorbed at time t and at equilibrium respectively and k_1 , k_2 are rate constants of the adsorption process of pseudo-first order and pseudo-second order. The equilibrium adsorption capacity (q_e) and the rate constant k_2 (g/mg.min) were determined with plot of (t/q_t) versus time. The fitting of these models is more often verified by the linear plots of $\ln(q_e - q_t)$ versus t , and t/q_t versus t , respectively. From the slope and intersection of the straight line, the corresponding constant values for the pseudo-first-order and pseudo-second-order kinetic models can be obtained, for each studied initial concentration, providing the respective kinetic constants, k_1 , k_2 , q_e and r_2 parameters. The correlation coefficient for the pseudo-second-order equation was better than the correlation coefficient for the pseudo-first-order equation Table 3. Thus, good linearity of the pseudo-second-order plots was revealed that the interactions would follow the second order kinetics. This meant that the pseudo-second-order kinetic model can describe the adsorption system studied in our work [31].

Conclusion

The adsorption of reactive dyes onto adsorbent AFP was a pH-dependent process with the maximum removal efficiency at the initial pH of 2-3. Thermodynamic studies suggested that adsorption reaction onto adsorbent AFP was an endothermic and spontaneous process. Langmuir isotherm described the equilibrium data of dyes on adsorbent AFP better than Freundlich isotherm. The adsorption capacities from the Langmuir isotherm were 34.13 and 11.33 mg/g for RR-23 and RB-19 at 22°C, respectively. Adsorption processes for reactive dyes were found to follow the pseudo second-order kinetics rate expression with intra particle diffusion as rate controlling mechanism. The present work revealed that the adsorbent AFP was a promising material for the removal of reactive dyes from aqueous solutions.

Acknowledgements-The authors thank the supervisory Board of Higher School of Textile and Clothing Industries (ESITH) for financial support and for its technical assistance.

References

1. Boer C. G., Obici L., Souza C. G. M., Piralta R. M. *Bioresour Technol.* 94 (2004) 107.
2. Maleki A., Mahvi A. H., Ebrahimi R., Zandsalimi Y. *J. Chem. Eng.* 9 (2010) 1805.
3. Kamal A. N. *J. Hazard. Mater.* 165 (2009)52.
4. Gupta V. K., Suhas I. A., Mohan D. *J. Colloid. Interface Sci.* 265 (2003) 257.
5. Forgacs E., Cserhatia T., Oros G. *Environ Int.* 30 (2004) 953.
6. Robinson T., McMullan G., Marchant R., Nigam P. *Bioresour. Technol.*77 (2001) 247.
7. Babel S., Opiso M. E. *Int. J. Environ. Sci. Tech.* 4 (2007) 99.
8. Abdel-Ghani N. T., Hefny M., El-Chaghaby G. A. F. *Int. J. Environ. Sci. Tech.*4(2006) 67.
9. Low K. S., Lee C. K., Tan K. K. *Bioresour. Tech.* 52 (1995) 79.
10. Annadurai G., Juang R., Lee D. *J. Hazard. Mater.* B92 (2002) 263.
11. Robinson T., Chandran B., Nigam P. *Bioresour. Technol.* 85 (2002) 119.
12. Ncibi M. C., Mahjoub B., Seffen M.. *Int. J. Environ. Sci. Tech.* 4 (2007) 433.
13. Ignat M.-E., Dulman V., Onofrei T. *Cellulose Chem. Technol.* 46 (2012) 357.
14. Akchich O., Marchak A. B., Butko Y. G. *Chemistry of plant raw materials.* (1987) 75.
15. Sun D., Zhang Z., Wang M., Wu Y. *Am. J. Anal. Chem.* 4 (2013) 17.
16. Gupta V. K., Rastogi A. *J. Hazard. Mater.* 163 (2009) 396.
17. Rahman M. S., Islam M. R. *Chem. Eng. J.* 149 (2009) 273.
18. Namasivayam C., Kanchana N., Yamuna R. T. *Waste Management* 1(1993) 33.
19. Sivaraj R., Namasivayam C., Kadirvelu K. *Waste management.* 21(2001) 105.
20. Rengaraj S., Joo C. K., Kim Y., Yi J. *J. Hazard Mater. B* 102 (2003) 257.
21. Lee I. H., Kuan Y.-C., Chern J.-M.. *J. Chin. Inst. Chem. Eng.* 38 (2007) 71.
22. Agrawal A., Sahu K. K., Pandey B. D. *Colloids Surf. A.* 23 (2004) 133.
23. McKay G. *J. Chem. Technol. Biotechnol.* 32 (1982) 759.
24. Boubberka Z., Kacha S., Kameche M., Elmaleh S., Derriche Z. *J Hazard Mater.* B119 (2005) 117.
25. Erika de Castro V., Danielle C., Joao Luiz Andreotti D., Anderson Marcos Dias C., Luciana I., Marcos, R., Agnes de Paula S. *Environ. Technol.* 35 (2014) 1532.
26. Raffiea Baseri J., Palanisamy P. N., Sivakumar P. *Int. J. Chem. Res.* 3 (2012) 36.
27. Webber T. N., Chakravarti R. K. *J Am. Inst. Chem. Eng.* 20 (1974) 228.
28. Poots V. J. P., McKay G., Healy J. J. *Water Pollut. Cont. Fed.* 50 (1978) 926.
29. Bakhshi Z., Najafpour G., Kariminezhad E., Pishgar R., Mousavi N., Taghizade T. *Environ. Technol.* 32 (2011) 1835.
30. Ho Y.S., Mckay G. *Proc. Biochem.*34 (1999) 451.
31. Tien C.T., Huang C. P. (Ed. *Vernet, J.P.*), Elsevier, Amsterdam, London, New York and Tokyo, (1991) 295-311.

(2015); <http://www.jmaterenvironsci.com>